Available online at www.sciencedirect.com
ScienceDirect
Nuclear Physics B Proceedings Supplement 00 (2012) 1–9
Nuclear Physics B Proceedings Supplement

Exclusive diffraction at HERA

Justyna Tomaszewska for the H1 and ZEUS collaborations

Deutsches Elektronen Synchrotoron, Notkestrasse 85, 22603 Hamburg, Germany

Abstract

Recent experimental results on diffractive vector meson production and deeply virtual Compton scattering from the H1 and ZEUS collaborations are reviewed.

Keywords:
vector mesons, DVCS, dipion, soft diffraction, hard difraction

1. Introduction

HERA was an electron-proton collider at DESY in Hamburg [1]. Electrons or positrons of 27.5 GeV were scattered on protons of 920 GeV (at the end of HERA operation - reduced to 575 GeV and 460 GeV). The center-of-mass energy was $\sqrt(s) = 318\,\text{GeV}$ ($\sqrt(s) = 252,\ 225\,\text{GeV}$).

1.1. Deep Inelastic Scattering

The scattering of electrons (positrons) off protons is one of the sources of our knowledge about fundamental processes. The ep interaction may proceed via the exchange of either a neutral boson, γ or Z^0 (neutral current) or a charged boson $W^{\pm}$ (charged current) [2]. Depending on the value of the four-momentum transfer squared, the ep interactions can be classified as deep inelastic scattering (DIS), where the electron scatters off the proton with a four-momentum-transfer squared (virtuality of the exchanged boson) sufficiently large to probe the proton at distances much smaller then its radius, or photoproduction, where a quasi-real photon is exchanged.

DIS may be described using the following variables: virtuality of the exchanged photon, Q^2, the Bjorken scaling variable, x, and the fraction of the electron momentum transferred to the proton in its rest system, y. These variables are not independent but are connected by the relation $Q^2 = x \cdot y \cdot s$.

1.2. Diffraction

In diffraction, no quantum numbers are exchanged. This processes can be described in the framework of Regge phenomenology as well as in perturbative Quantum Chromodynamics (pQCD).

In Regge theory [3], the exchanged object between the proton and the diffractive system X is a 'Regge trajectory', which is parametrized to be linear,

$$\alpha_R(t) = \alpha_R(0) + \alpha' \cdot t\ .$$

In the case when the trajectory carries the quantum numbers of the vacuum, it is called the Pomeron trajectory [4] and the exchanged object - the Pomeron. Diffractive cross-sections at high energies can be parametrized as a function of the photon-proton center-of-mass energy,W, as well as a function of the four-momentum transferred squared at the proton vertex, t, and can be written in the form:

$$\frac{d\sigma}{dt} \propto e^{b(W)\cdot t}\left(\frac{W}{W_0}\right)^{4(\alpha_P(t)-1)}$$

$$\sigma_{tot} \propto \left(\frac{W}{W_0}\right)^{2(\alpha_P(0)-1)}$$

$$\text{with}\quad b(W) = b_0 + 4\alpha' \cdot ln\left(\frac{W}{W_0}\right) \cdot t\ .$$

From a fit to all peripheral hadronic scattering and total cross-section data Donnachie and Landshoff [5]

found the following universal parametrization of the Pomeron trajectory :

$$\alpha_{I\!P}(t) = 1.08 + 0.25 \cdot t.$$

Processes which are described by this trajectory are called soft diffraction processes. The predictions from Regge theory for soft diffraction are a power law behavior of the cross section as $\sigma(W) \propto W^{\delta}$ with $\delta \approx 0.22$ and an exponential drop of the differential cross section as a function of t with an increasing slope, $b(W)$, as W increases.

This last fact is called shrinkage. The slope parameter b is proportional to r^2, where r is a measure for the extension of the interacting objects. With increasing W also r increases which means that the scattering objects get bigger.

In hard diffraction, the virtual photon splits into a quark-antiquark pair and, in the simplest approach, two gluons which form a colorless object are emitted from the proton and couple to the quark-antiquark pair. In higher orders of pQCD, the exchanged gluon system is commonly treated as a BFKL-type ladder [6]. Various pQCD inspired models exist for hard diffractive scattering. All these models predict little or no shrinkage.

Ideal processes to study the transition from soft to hard diffraction are exclusive production of Vector Meson and Deeply Virtual Compton Scattering (DVCS).

1.3. Exclusive Vector Meson Production

At high-energies, exclusive production of vector meson (V), $ep \rightarrow eVY$, where Y denotes the system into which the proton dissociates, can be described in terms of the Vector Dominance Model (VDM) [7] plus Regge theory providing a framework in which exclusive vector-meson production is understood as a quasi-elastic scattering where the incoming vector-meson is off mass-shell. The situation is graphically shown in Fig. 1.

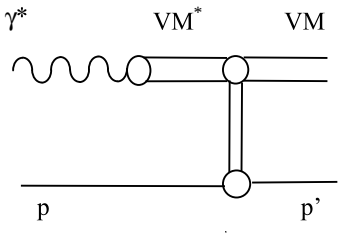

Figure 1: Exclusive vector-meson production in the VMD-Regge framework.

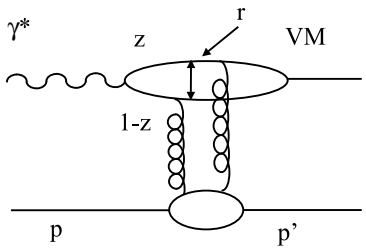

Figure 2: Exclusive vector-meson production as a pQCD process.

In pQCD, exclusive vector-meson production proceeds according to Fig. 2. The virtual photon splits into a quark-antiquark pair with relative momentum fractions z and $1 - z$. In lowest order, two gluons are exchanged between the proton and the quark-antiquark pair which recombines afterwards to form the vector-meson. The transverse separation, r, of the quark and antiquark is given in pQCD by :

$$r^2 = [z(1 - z)Q^2 + m_q^2]^{-1} .$$

Here m_q is the mass of the quark(antiquark) of which the vector-meson is composed. Perturbative QCD is expected to be applicable when the transverse dimension, r, of the quark-antiquark system gets small. This happens when either Q^2 or m_q get big. pQCD models predict a rise of the cross-section like $\sigma(W) \propto W^{\delta}$ with $\delta \approx 0.8$ which is faster than expected from Regge theory. The slope of the t-distribution is predicted to be $b \approx 4$ GeV and $\alpha' \approx 0$. This means no or little shrinkage. The conditions under which exclusive vector-meson production is a hard diffractive process that can be described by pQCD models will be investigated in the rest of this section.

1.4. Deeply Virtual Compton Scattering

The DVCS process is similar to diffractive vector meson production, where in the final state a real photon is observed instead of the vector meson. In lowest order of pQCD calculations, this exchange involves two gluons in a colourless configuration with different longitudinal and transverse momenta. These unequal momenta arise as a consequence of the mass difference between the incoming virtual photon and the outgoing real photon. The DVCS amplitude factorizes into a hard-scattering part, calculable in pQCD and a soft part which can be absorbed into the general patron distributions (GPDs) [8]. The cross section at sufficiently large Q^2 is expected to rise steeply with increasing W, due to the rise of the parton densities in the proton towards

small values of the Bjorken scaling variable x.

The exclusive production of the vector mesons ρ, ω, ϕ, J/ψ, ψ' and Υ [9, 10, 11, 12, 13, 14, 15] as well as Deeply Virtual Compton Scattering (DVCS) [16, 17] have been studied by the H1 and ZEUS experiments. The data from both experiments allow to investigate the transition from soft to hard regimes as a function of the various scales, M_V, t and Q^2.

2. δ dependence as a function of invariant-mass

The transition from the soft to the hard regime has been observed by studying the energy dependence of the cross section for different vector mesons in elastic photoproduction processes. The results are compiled in Fig. 3. The W-dependence of the cross section of the light vector-mesons (ρ, ω, ϕ) is described by Regge phenomenology. For higher mass vector mesons, the rise of the cross section with W gets steeper. This indicates the on-set of hard diffractive scattering.

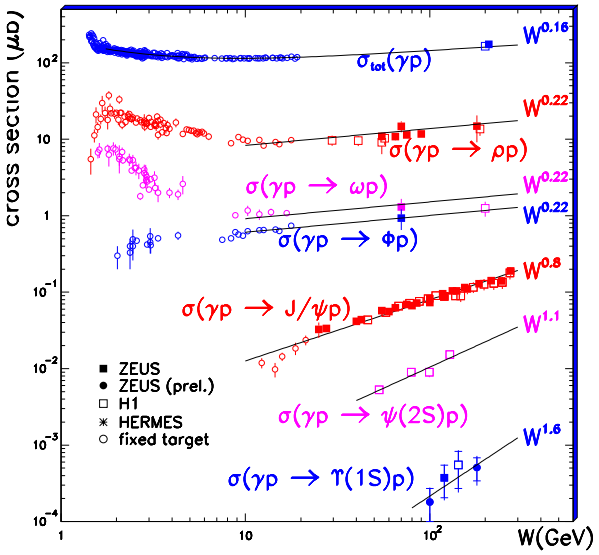

Figure 3: Cross sections as a function of $W_{\gamma p}$ of elastic photoproduction of ρ, ω, ϕ, J/ψ,ψ' and Υ vector mesons. The solid lines are functions of W^{δ} [18].

The H1 experiment has measured the exclusive photoproduction of J/ψ as a function of W for nominal and reduced energy in the centre-of-mass (Fig. 4) [19]. This allows to extend the phase-space toward lower W values. The measured cross section has been fitted with the function W^{δ}, resulting in a value $\delta = 0.81 \pm 0.08$, in good agreement with earlier measurements, indicating that the process is hard.

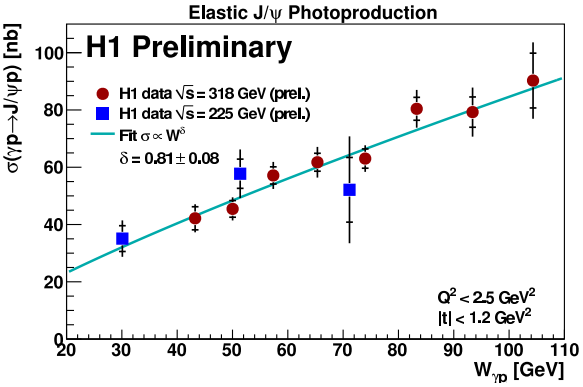

Figure 4: The cross section as a function of $W_{\gamma p}$ for elastic J/ψ photoproduction.

In the same experiment, the H1 collaboration also measured the energy dependence of the cross section for the proton-dissociation process, (Fig. 5), and obtained a value $\delta = 0.55 \pm 0.09$.

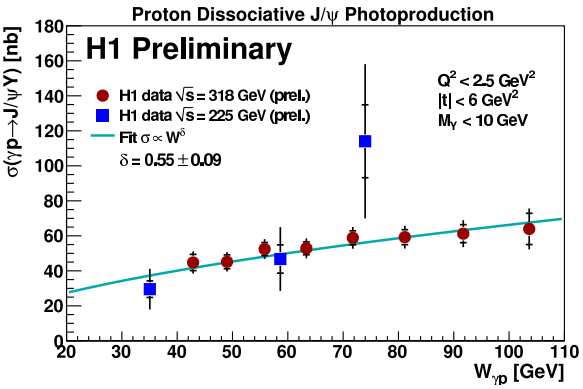

Figure 5: The cross section as a function of $W_{\gamma p}$ for proton dissociative J/ψ photoproduction.

The pQCD description of high mass photoproduction has also been confirmed by the ZEUS collaboration in the measurement of the Υ cross section. The results are presented in Fig. 6. The steep energy dependence predicted by pQCD inspired models is borne out by the data.

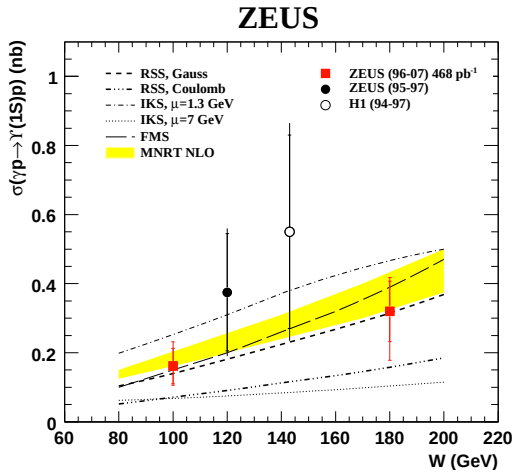

Figure 6: The cross section as a function of $W_{\gamma p}$ for Υ photoproduction.

3. δ dependence as a function of Q^2

The transition from soft to hard regime can be investigated by varying Q^2 for a given vector meson. The following results have been provided for the light vector meson ρ by the H1 (Fig. 7) and the ZEUS (Fig. 8) experiments.

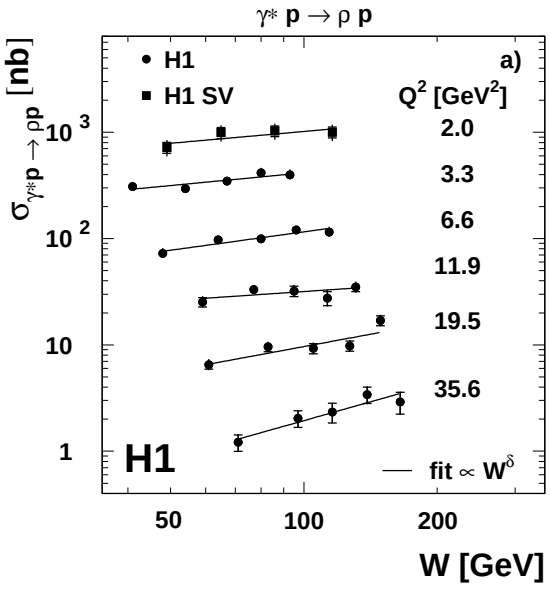

Figure 7: W dependence of the $\gamma^* p$ cross sections for elastic ρ meson production at different Q^2 values, as measured by the H1 collaboration. The lines are the results of the power law fits.

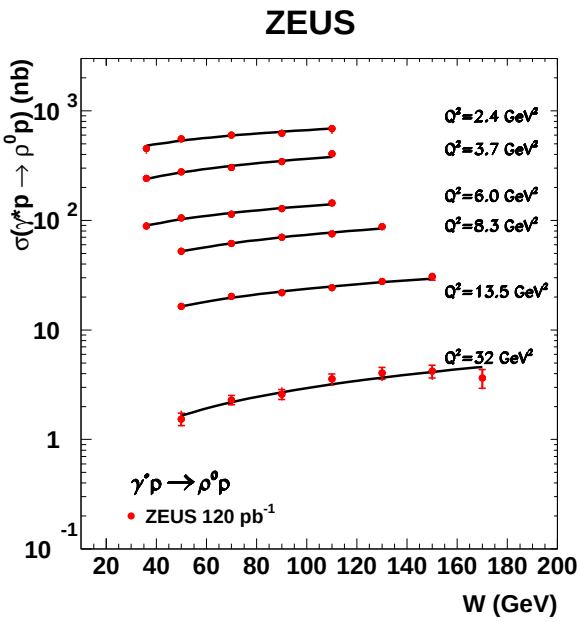

Figure 8: The cross section as a function of $W_{\gamma p}$ for elastic ρ meson production at different Q^2 values, as measured by the ZEUS collaboration. The lines are the results of the power law fits.

The W dependence becomes steeper with increasing Q^2. The W dependence is parametrized by a power law function, and the results of the fit are compiled in Fig. 9. The value of δ increases with $Q^2 + M^2$ to the value obtained for heavy vector mesons.

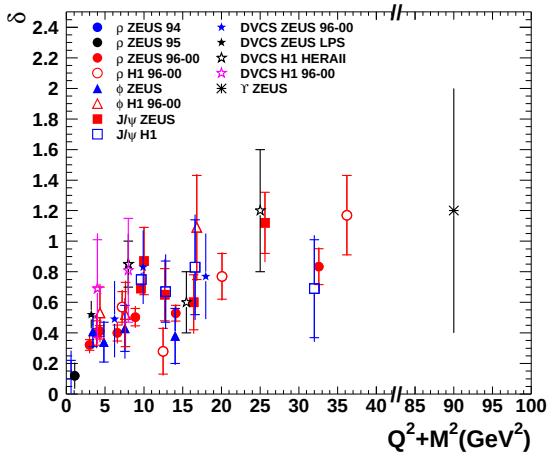

Figure 9: The value of the δ parameter for a selection of vector mesons and DVCS, as a function of $Q^2 + M^2$

The transition from soft to hard regime can also be measured in the DVCS process. The $\gamma^* p$ DVCS cross section, $\sigma^{\gamma^* p\to\gamma p}$, as a function of W for the H1 and the ZEUS experiments is presented in Fig. 10 and Fig. 11, respectively. The data have been fitted with the function W^δ, and the results of this fit are collected in Fig. 12.

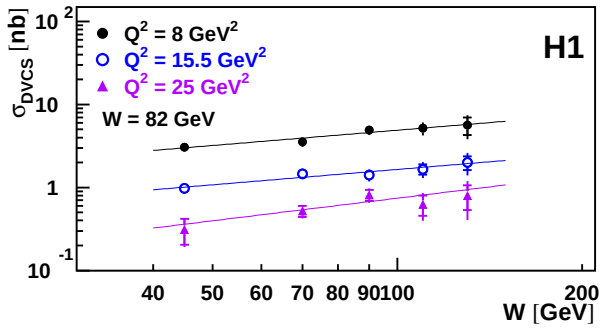

Figure 10: The DVCS cross section as a function of W at three values of Q^2. The solid lines represent the results of fits of the form W^δ. The inner error bars represent the statistical errors, the outer error bars the statistical and systematic errors added in quadrature [16].

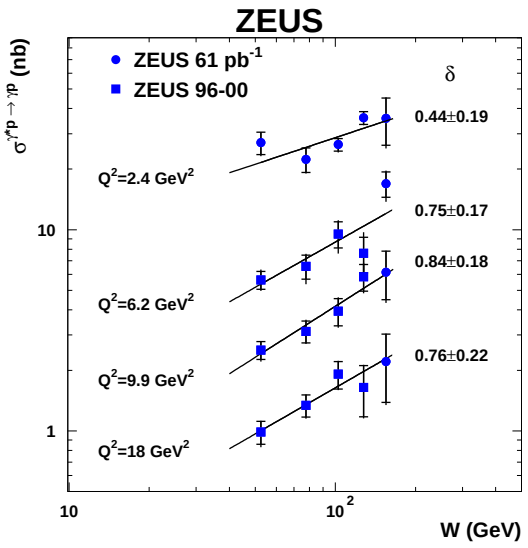

Figure 11: The DVCS cross section, $\sigma^{\gamma^* p\to\gamma p}$, as a function of W. The solid lines are the results of a fit of the form $\sigma^{\gamma^* p\to\gamma p} \propto W^\delta$. The values of δ and their statistical uncertainties are given in the figure. The inner error bars represent the statistical uncertainty, the outer error bars the statistical and systematic uncertainties added in quadrature [17].

Within the present accuracy the results do not show evidence for a Q^2 dependence of δ. This result is similar to that obtained for the exclusive production of J/ψ .

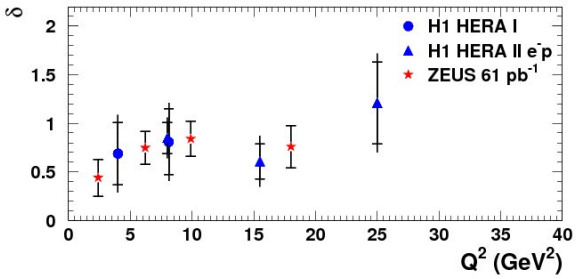

Figure 12: The δ values from DVCS as a function of Q^2 for the H1 and ZEUS experiments. The inner error bars represent the statistical uncertainty, the outer error bars the statistical and systematic uncertainties added in quadrature.

4. t dependence

The differential cross section, $d\sigma/dt$, has been parametrized by an exponential function e^{bt}, where the b slope determines the size of the interactions region which depends on the proton radius and on the size of the produced vector meson. In case of photoproduction of light vector mesons, the photon is large and so is the vector meson. Thus one expects a large value for the slope. As the scale gets larger, either Q^2 or the vector-meson mass, b gets smaller and measures the size of the proton. Below are presented some recent measurements of the slopes of Υ, J/ψ and DVCS.

4.1. Photoproduction of Υ

The measured $|t|$ distribution for exclusive Υ photoproduction is presented in Fig. 13.

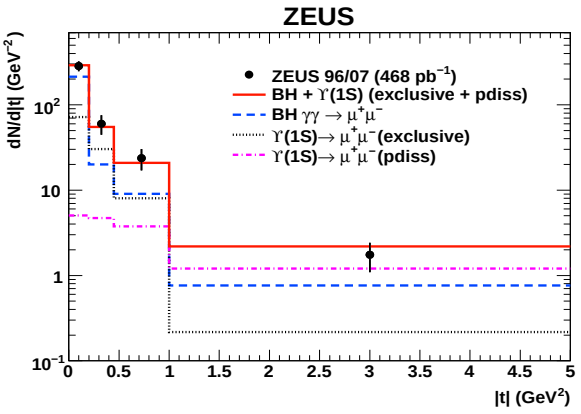

Figure 13: Measured $|t|$ distribution (full dots) with error bars denoting statistical uncertainties. Fitted distributions for simulated events are shown for the Bethe-Heitler (dashed line), exclusive $\Upsilon(1S)$ (dotted line) and proton dissociative $\Upsilon(1S)$ (dashed-dotted line) processes. The solid line shows the sum of all contributions [20].

The value of the slope parameter for exclusive $\Upsilon(1S)$ has been determined. The contribution of all processes was obtained by using simulated distributions [20]. Due to insufficient statistics it was not possible to evaluate the contribution of proton-dissociative $\Upsilon(1S)$ events in the final sample with the present data. However, the fraction of such events, $f_{\rm pdiss}$, is expected to be similar in all diffractive vector-meson production processes [21]. Therefore, a value $f_{\rm pdiss} = 0.25 \pm 0.05$, determined for diffractive J/ψ production [22], was used. The values of the slope parameters for exclusive and proton dissociative $\Upsilon(1S)$ production processes differ [23]; in the MC the value for the latter was taken to be $b_{\rm pdiss} = 0.65 \pm 0.1$ GeV^{-2} [22]

The fit was performed with two free parameters, the slope b and the number of expected $\Upsilon(1S)$ events in the signal mass window. During the parameter scan, the contribution of the exclusive $\Upsilon(1S)$ production to the t distribution was reweighted at the generator level to the function $b \cdot \exp(-b|t|)$. The fit yielded: $b = 4.3^{+2.0}_{-1.3}$ (stat.) GeV^{-2} and 41 ± 10 $\Upsilon(1S)$ events (44% of the events in this mass window). The value of b is in good agreement with expectations of pQCD models.

4.2. Photoproduction of J/ψ

The t dependence of the elastic cross section of J/ψ meson photoproduction for nominal elastic (Fig. 14) and proton dissociation (Fig. 15) as well as for the elastic process at a reduced energy (Fig. 16)) has been studied by the H1 experiment.

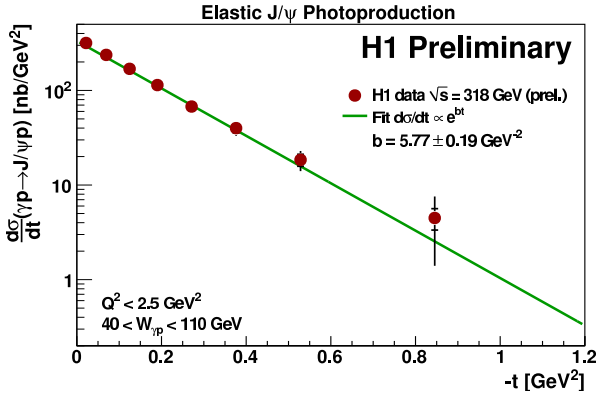

Figure 14: The J/ψ cross section as a function of $-t$ for elastic events in photoproduction.

For elastic production of J/ψ the cross section has been parametrized with the exponential function e^{-bt}. The value of the slope b, has been measured as $b = 5.77 \pm 0.19$ GeV^{-2} and $b = 4.75 \pm 0.5$ GeV^{-2} for nominal and reduced energy of the proton beam, respectively. This shows a slight dependence of the b slope on W.

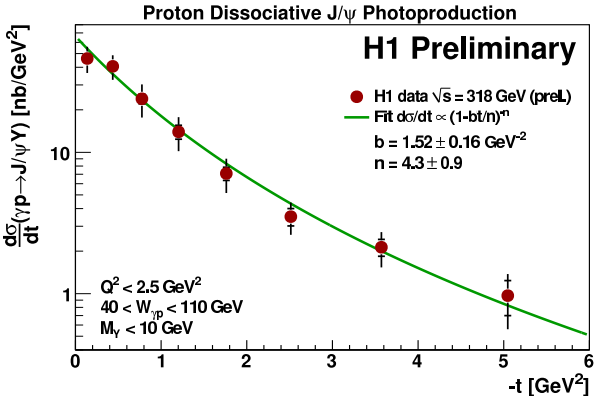

Figure 15: The J/ψ cross section as a function of $-t$ for proton-dissociative events in photoproduction.

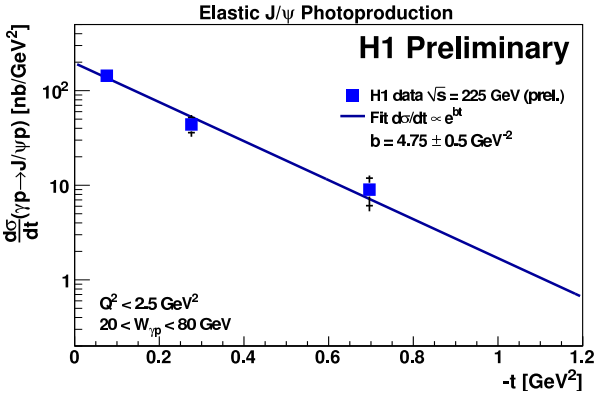

Figure 16: The J/ψ cross section as a function of $-t$ for elastic events in photoproduction.

The differential cross section for the proton-dissociative process as a function of $-t$ has been parametrized as $(1 - bt/n)^{-n}$, where n is a power law. It shows the exponential behaviour at low $|t|$ and follows a power law at larger $|t|$. As expected, the proton-dissociative process has a much shallower t dependence than the elastic process.

4.3. DVCS

The first direct measurement of the DVCS differential cross section as a function of $|t|$ has been measured by tagging the outgoing proton using the leading proton spectrometer (LPS) [24]. The data are presented in Fig. 17 and fitted with the function e^{-bt}.

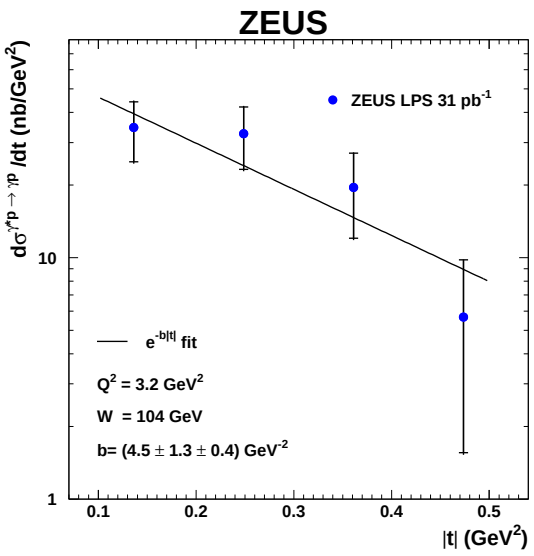

Figure 17: The DVCS differential cross section, $d\sigma^{\gamma^* p\to\gamma p}/dt$, as a function of $|t|$. The solid line is the result of a fit of the form $\sim e^{-b|t|}$. The inner error bars represent the statistical uncertainty, the outer error bars the statistical and systematic uncertainties added in quadrature.

The resulting value of the slope b has been obtained as $4.5 \pm 1.3 \pm 0.4$. In spite of the low acceptance and therefore low statistics data, this is a very clean measurement due to the absence of proton dissociation. The value obtained from this direct measurement is compared in Fig. 18 with those from indirect measurements by the H1 experiment at a few Q^2 values. The slopes show no Q^2 dependence.

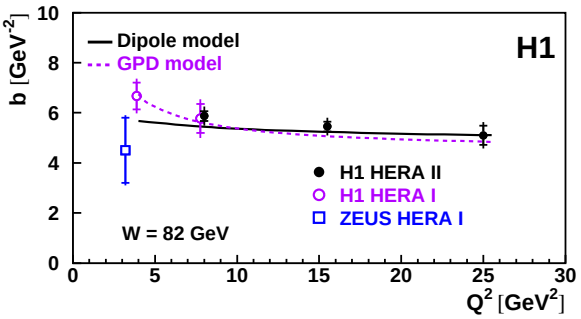

Figure 18: The fitted t-slope parameters $b(Q^2)$ for DVCS are shown together with the t-slope parameters from the previous H1 [25] and ZEUS [17] publications based on HERA I data.

A compilation of the b slope values obtained by both HERA experiments for different vector mesons and for DVCS are presented in Fig. 19 as a function of $M^2 + Q^2$. The value of b decreases to an asymptotic value of $\sim 5\,\mathrm{GeV}^{-2}$. This is a measure of the radius of the gluons density in the proton and translates to a size of about 0.6 fm. This values is smaller than the value of the electromagnetic radius of the proton (around 0.8 fm).

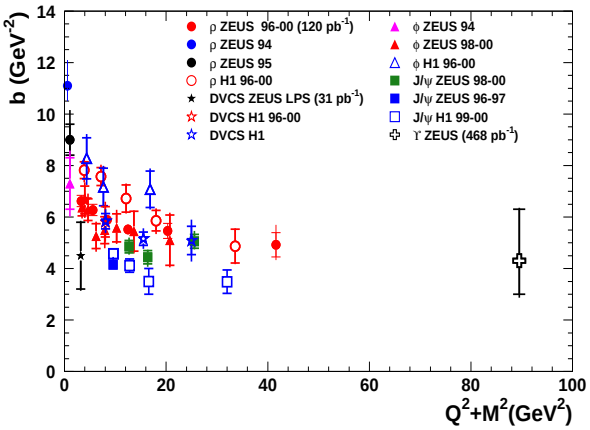

Figure 19: A compilation of b slope values for selected vector mesons and for DVCS.

5. Exclusive Dipion Production

The exclusive diffractive production of vector mesons gives not only information about the transition from the soft to the hard region, but can also be a source of information about the electromagnetic pion form factor. The electromagnetic pion form factor, $F_\pi(M_{\pi\pi})$, can be related to the $\pi\pi$ invariant-mass distribution through the following relation [26, 27]:

$$\frac{dN(M_{\pi\pi})}{dM_{\pi\pi}} \propto |F_\pi(M_{\pi\pi})|^2$$

In the mass range $M_{\pi\pi} < 2.5$ GeV, Kuhn-Santamaria (KS) [28] include contributions from the $\rho(770)$, $\rho'(1450)$ and $\rho''(1700)$ resonances,

$$F_\pi(M_{\pi\pi}) = \frac{BW_\rho(M_{\pi\pi}) + \beta BW_{\rho'}(M_{\pi\pi}) + \gamma BW_{\rho''}(M_{\pi\pi})}{1+\beta+\gamma}.$$

Here β and γ are relative amplitudes and BW_V is the Breit-Wigner distribution of the vector meson V.

The $\pi^+\pi^-$ mass distribution, after acceptance correction, is shown in Fig. 20. A clear peak is seen in the ρ mass range. A small shoulder is apparent around 1.3 GeV and a secondary peak at about 1.8 GeV.

The two-pion invariant-mass distribution was fitted, using the least-square method [29], as a sum of two terms,

$$\frac{dN(M_{\pi\pi})}{dM_{\pi\pi}} = A\left(1-\frac{4M_\pi^2}{M_{\pi\pi}^2}\right)\left[|F_\pi(M_{\pi\pi})|^2 + B\left(\frac{M_0}{M_{\pi\pi}}\right)^n\right],$$

where A is an overall normalization constant. The second term is a parameterization of the non-resonant background, with constant parameters B, n and $M_0 = 1$ GeV. The other parameters, the masses and widths of the three resonances and their relative contributions β and γ, enter through the pion form factor, F_π. The fit, which includes 11 parameters, gives a good description of the data. The result of the fit is shown in Fig. 20 together with the contribution of each of the two terms. The ρ and the ρ'' signals are clearly visible. The negative interference between all the resonances results in the ρ' signal appearing as a shoulder.

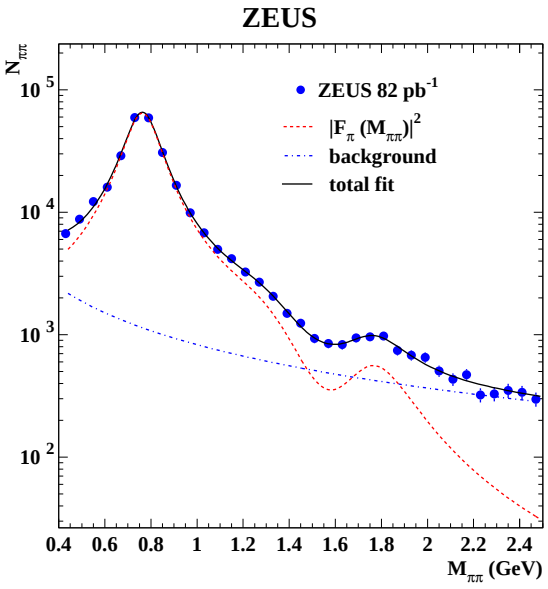

Figure 20: The two-pion invariant-mass distribution, $M_{\pi\pi}$, where $N_{\pi\pi}$ is the acceptance-corrected number of events in each bin of 60 MeV. The dots are the data and the full line is the result of a fit using the Kuhn-Santamaria parameterization. The dashed line is the result of the pion form factor normalized to the data, and the dash-dotted line denotes the background contribution.

5.1. Q^2 dependence of the pion form factor

The Q^2 dependence of the relative amplitudes was determined by performing the fit to $M_{\pi\pi}$ in three Q^2 regions, 2–5, 5–10 and 10–80 GeV^2. The results are shown in Fig. 21. A reasonable description of the data is achieved in all three Q^2 regions. The absolute value of β increases with Q^2, while the value of γ is consistent with no Q^2 dependence, within large uncertainties.

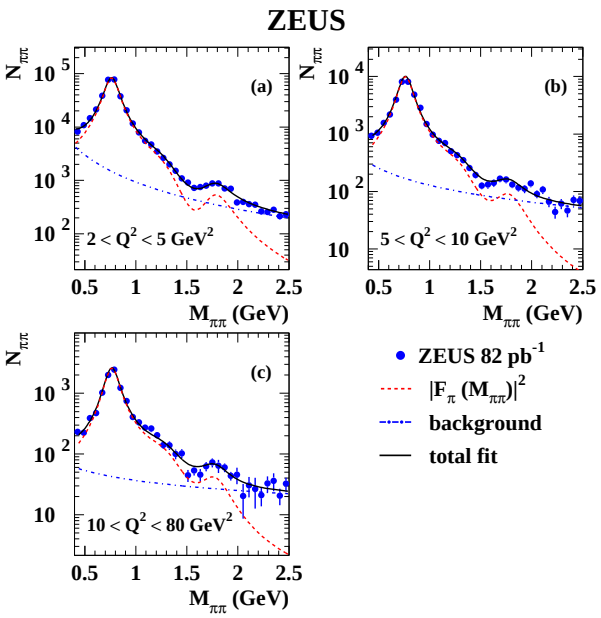

Figure 21: The two-pion invariant-mass distribution, $M_{\pi\pi}$, where $N_{\pi\pi}$ is the acceptance-corrected number of events in each bin of 60 MeV, for three regions of Q^2, as denoted in the figure. The dots are the data, and the full line is the result of a fit using the Kuhn-Santamaria parameterization. The dashed line is the result of the pion form factor normalized to the data, and the dash-dotted line denotes the background contribution.

5.2. Cross-section ratios as a function of Q^2

The Q^2 dependence of the ρ by itself is given elsewhere [10]. Since the $\pi\pi$ branching ratios of ρ' and ρ'' are poorly known, the ratio R_V defined as

$$R_V = \frac{\sigma(V)\cdot Br(V\to\pi\pi)}{\sigma(\rho)},$$

has been measured, where σ is the cross section for vector-meson production, and $Br(V \to \pi\pi)$ is the branching ratio of the vector meson $V(\rho', \rho'')$ into $\pi\pi$.

The ratio R_V for $V = \rho', \rho''$, as a function of Q^2 is presented in Fig. 22. Owing to the large uncertainties of $R_{\rho''}$, no conclusion on its Q^2 behaviour can be deduced, whereas $R_{\rho'}$ clearly increases with Q^2. This rise has been predicted by several models [30, 31, 32, 33, 34]. The suppression of the $2S$ state (ρ') is connected to a node effect, which results in cancellations of contributions from different impact-parameter regions at lower Q^2, while at higher Q^2 the effect vanishes.

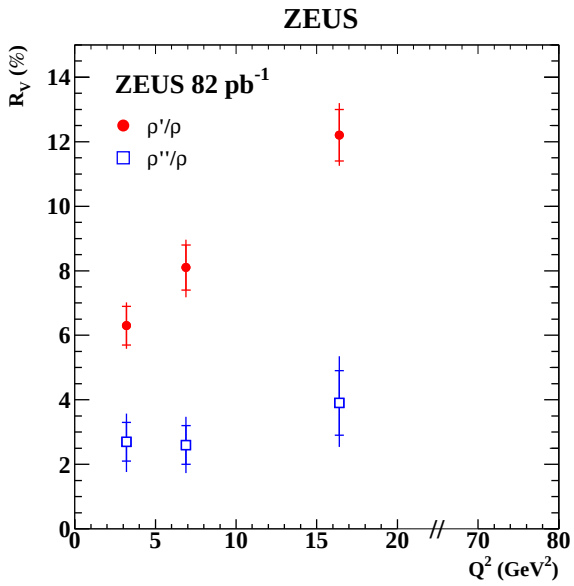

Figure 22: The ratio R_V as a function of Q^2 for $V = \rho'$ (full circles) and ρ'' (open squares). The inner error bars indicate the statistical uncertainty, the outer error bars represent the statistical and systematic uncertainty added in quadrature.

References

[1] "A Proposal for a Large Electron-Proton Colliding Beam Facility at DESY," DESY HERA 81-10 (1981).

[2] M. Derrick *et al.* [ZEUS Collaboration], Phys. Rev. Lett. 75 (1995) 1006 [hep-ex/9503016].

[3] T. Regge, Nuov. Cim. 14 (1959) 951, Nuov. Cim. 18 (1960) 947; P. Collins, "An Introduction to Regge Theory and High Energy Physics", Cambridge University Press, Cambridge (1977).

[4] G. Chew and S. Frautschi, Phys. Rev. Lett. 7 (1961) 394; N. Gribov, Sov. Phys. JETP 14 (1962) 478, ibid. 1395.

[5] A. Donnachie and P.V. Landshoff, Nucl. Phys. 244 (1984) 322, Phys. Lett. B 296 (1992) 227.

[6] L.N. Lipatov, Sov. J. Nucl. Phys. 23 (1976) 338; E.A. Kuraev, L.N. Lipatov and V.S. Fadin, Sov. Phys. JETP 45 (1977) 199; Y.Y. Balitsky and L.N. Lipatov, Sov. J. Nucl. Phys. 28 (1978) 822.

[7] J.J. Sakurai, "Currents and Mesons", University of Chicago Press, Chicago (1969); H. Fraas and D. Schildknecht, Nucl. Phys. B 14 (1969) 543.

[8] L.L. Frankfurt, A. Freund and M. Strikman, Phys. Rev. D 58 (1998) 114001, Erratum ibid. D 59 (1999) 119901; X. Ji, Phys. Lett. B 78 (1997) 610; K. Golec-Biernat and A. Martin, Phys. Rev. D 59 (1999) 14029.

[9] F.D. Aaron *et al.* [H1 Collaboration], JHEP 05 (2010) 032.

[10] S. Chekanov *et al.* [ZEUS Collaboration], PMC Phys. A 1 (2007) 6.

[11] J. Breitweg *et al.* [ZEUS Collaboration], Phys. Lett. B 487 (2000) 273; M. Derrick *et al.* [ZEUS Collaboration], Z. Phys. C 73 (1996) 73.

[12] S. Chekanov *et al.* [ZEUS Collaboration], Nucl. Phys. B 718 (2005) 3; M. Derrick *et al.* [ZEUS Collaboration], Phys. Lett. B 377 (1996) 259.

[13] A. Aktas *et al.* [H1 Collaboration], Eur. Phys. J. C 46 (2006) 585.

[14] S. Chekanov *et al.* [ZEUS Collaboration], Nucl. Phys. B 695 (2004) 3, Eur. Phys. J. C 24 (2002) 345.

[15] S. Chekanov *et al.* [ZEUS Collaboration], Phys. Lett. B 680 (2009) 4.

[16] F.D. Aaron *et al.* [H1 Collaboration], Phys. Lett. B 681 (2009) 391.

[17] S. Chekanov *et al.* [ZEUS Collaboration], JHEP 0905 (2009) 108.

[18] ZEUS Coll., "Exclusive Photoproduction of Upsilon Mesons at HERA," ZEUS-prel-07-015, presented at EPS07, 2007.

[19] H1 Coll., "Exclusive Photoproduction of J/ψ Mesons at HERA," H1-prel-11-011.

[20] H. Abramowicz *et al.* [ZEUS Collaboration], "Measurement of the t dependence in exclusive photoproduction of Upsilon(1S) mesons at HERA," arXiv:1111.2133 [hep-ex].

[21] J. Breitweg *et al.* [ZEUS Collaboration], Eur. Phys. J. C 14 (2000) 213.

[22] S. Chekanov *et al.* [ZEUS Collaboration], Eur. Phys. J. C 24 (2002) 345.

[23] F.D. Aaron *et al.* [H1 Collaboration], JHEP 1005 (2010) 032.

[24] M. Derrick *et al.* [ZEUS Collaboration], Z. Phys. C 73 (1997) 253 [hep-ex/9609003].

[25] A. Aktas *et al.* [H1 Collaboration], Eur. Phys. J. C 44 (2005) 1 [arXiv:hep-ex/0505061].

[26] B. Clerbaux and M.V. Polyakov, Nucl. Phys. A 79 (2000) 185.

[27] M.V. Polyakov, Nucl. Phys. B 555 (1999) 231.

[28] J.H. Kuhn and A. Santamaria, Z. Phys. C 48 (1990) 445.

[29] F. James *et al.*, MINUIT, CERN DD/D506, 1994.

[30] J. Nemchik, N.N. Nikolaev and B.G. Zakharov, Phys. Lett. B 339 (1994) 194.

[31] L. Frankfurt, W. Koepf and M. Strikman, Phys. Rev. D 54 (1996) 3194.

[32] I.P. Ivanov and N.N. Nikolaev, Acta Phys. Polon. B 33 (2002) 3517.

[33] H. Abramowicz, L. Frankfurt and M. Strikman, Surveys High Energy Phys. 11 (1997) 51.

[34] I.P. Ivanov, PhD Thesis (Bonn University), hep-ph/0303035 (2003).